Secondary Nucleation of Aβ Fibrils on Liposome Membrane

Toshinori Shimanouchi, Nachi Kitaura, Ryo Onishi, Hiroshi Umakoshi, and Ryoichi Kuboi
Division of Chemical Engineering, Graduate School of Engineering Science, Osaka University,
1-3 Machikaneyama-cho, Toyonaka, Osaka 560-8531, Japan

DOI 10.1002/aic.13772
Published online March 12, 2012 in Wiley Online Library (wileyonlinelibrary.com).

The amyloid fibrils of amyloid β protein (Aβ) from Alzheimer's disease are likely to show the cytotoxicity, depending on their morphology. The relationship between the nucleation kinetics of the Aβ fibrils and their morphology has been investigated. From the perspective of a crystallization technique assuming primary/secondary nucleation steps and an elongation step, the secondary nucleation rate B *[# m^{-3} s^{-1}], was experimentally and coarsely determined by using total internal reflection fluorescence microscopy combined with thioflavin* T. *In an aqueous solution, linear and rigid fibrils were formed with a relatively smaller* B *value ($(2.83 \pm 0.55) \times 10^5$ # m^{-3} s^{-1}), whereas spherulitic amyloid assemblies were formed in the presence of negatively charged liposome including oxidized lipids, with a larger* B *value ($(7.65 \pm 0.47) \times 10^5$ # m^{-3} s^{-1}). Those findings should lead to a better understanding of the mechanism for the formation of fibrils and senile plaques in Alzheimer's disease.* © 2012 American Institute of Chemical Engineers *AIChE J*, 58: 3625–3632, 2012
Keywords: biocrystallization, crystal morphology, proteins

Introduction

Alzheimer's disease (AD) is a progressive neurodegenerative disease characterized by extracellular amyloid plaques and interneuronal fibrillary tangles in the brain.[1–3] The amyloid plaques are mainly composed of amyloid β protein (Aβ), which is a 40- to 43-amino acid product and is secreted from the amyloid precursor protein.[1] The formation of fibrillar aggregate by Aβ has been widely investigated, both in aqueous solution[4] and in the presence of model biomembranes.[5] Recent reports imply that small species such as oligomers,[6] filaments, and protofibrils,[7] which are formed during the amyloid fibril formation of Aβ, could be a key factor in determining its cytotoxicity. It has been reported, for the matured fibrils, that their morphology could also be a key factor in determining its cytotoxicity.[8] Although the spherulitic amyloid assemblies of Aβ have been reported to be formed as a model senile plaque,[9] the mechanism to form the Aβ fibrils with various shapes has not yet been clarified. A clarification of this mechanism would result in a better understanding of the role of Aβ in AD.

The morphology of the amyloid fibrils has previously been observed by using scanning electron microscopy (SEM)[10] or total internal reflection fluorescence microscopy (TIRFM).[9,11] The SEM and TIRFM have clearly revealed a variety of morphologies of the amyloid fibrils such as linear and rigid fibrils[9,11] or spherulitic amyloid assemblies (spherulite).[10] Recently, it has been qualitatively shown that laser irradiation of the fibrils can induce the formation of spherulitic amyloid assemblies and their explosive proliferation,[11] and it has been proposed that the laser irradiation induces the fragmentation of amyloid fibrils. Lundbury Jr and coworkers[12] have reported that fibril formation occurs by one-dimensional (1-D) crystallization. Actually, fibril formation involves common phenomena occurring in conventional crystallization, including nucleation,[3,13–15] elongation,[3,13,14,16,17] secondary nucleation,[18] and polymorphism.[14,19] The secondary nucleation is herein defined the fragmentation or aggregation of original fibrils,[18] which follows the formation of small species of amyloids such as protofibrils or filaments. It is, therefore, possible that the formation of spherulitic amyloid assemblies can be quantitatively analyzed by a method to estimate the secondary nucleation. These approaches would shed light on a hidden mechanism for the induction of fibrils with a variety of morphologies.

A biomembrane could be a possible key material to differentiate the morphology of the amyloid fibrils because it is a principle component of the biological cell (i.e., neural cell). It has been revealed that the structures of fibrils formed in the presence of model biomembrane (liposomes) are different from those of fibrils formed in aqueous solution.[5] In our series of studies, it was shown that a model biomembrane (liposome) with a designed surface could recognize the biomolecules (i.e., peptide, nucleoside), and could convert their conformation and/or assembly, resulting in the creation of new value (enzyme-like function (LIPOzyme), gene-regulation, etc.).[20] Especially in the case of amyloid fibril formation, there have been some reports regarding the possible regulatory role of liposome membranes[5] and supported phospholipid bilayers[21] in the fibril formation of Aβ. It is, therefore, important to study amyloid fibril formation in a model biomembrane in order to understand the mechanisms of amyloid fibril formation *in vivo*.

In this study, the secondary nucleation rate B, was experimentally determined by employing the analytical method of secondary nucleation, which has commonly been applied in

Correspondence concerning this article should be addressed to H. Umakoshi at MSB@cheng.es.osaka-u.ac.jp.

the special research field of "*crystallization*", considering an analogy between Aβ fibril formation and the crystallization of small molecules. The formation of Aβ fibrils was kinetically studied with and without various liposomes by using a TIRFM method combined with thioflavin T (ThT), which can specifically bind to the fibrils. The possible role of liposome membrane in the differentiation of the morphology of the Aβ fibrils is finally discussed based on the estimated *B* value and direct observation of the corresponding morphology.

Materials and Methods

Materials

Amyloid-β protein with 40 amino acid residues (Aβ (1-40)) was purchased from the Peptide Institute (Osaka, Japan). 1,2-Dimyristoyl-*sn*-glycero-3-phosphocholine (DMPC), 1,2-dimyristoyl-*sn*-glycero-3-[phospho-*rac*-(1-glycerol)] (DMPG), 1,2-dimyristoyl-phosphatidic acid (DMPA), and 1-stearoyl-2-arachidonyl-*sn*-glycero-3-phosphocholine (SAPC) were obtained from Avanti Polar Lipids (Alabaster, AL, USA). Thioflavin T (ThT), NaCl, 2-Amino-2-hydroxylmethyl-1,3-propanediol, (Tris) and NH_3 were purchased from Wako Pure Chemical Industries, Ltd. (Japan Osaka). Ethylenediamine-*N*,*N*,N′,N′-tetra acetic acid,tetra sodium salt,tetra hydrate (EDTA) was obtained from Dojindo (Kumamoto, Japan). Other used reagents were purchased from Sigma Aldrich and Wako Pure Chemical Industries, Ltd. (Japan Osaka).

Preparation of Liposome

Preparation of nonoxidized liposome (DMPC, DMPA and DMPG liposome)

The liposome composed of DMPC, DMPA, or DMPG was prepared by a previously reported method.[22] The lipid was dissolved in chloroform and then dried by rotary evaporation under reduced pressure. The remaining solvent was removed under high vacuum overnight. The lipid was hydrated with water to form multilamellar vesicles (MLVs). Large unilamellar vesicles (LUVs) were formed from the MLVs with five cycles of freeze–thaw treatment. They were extruded through a polycarbonate filter with a 100-nm pore dia. using the extrusion device Liposofast from Avestin (Ottawa, Canada).

Preparation of oxidized liposome

The oxidized liposome was prepared by a previously reported method.[22] For the oxidization of SAPC, the $CuCl_2$ (2mM) and H_2O_2 (20mM) were added to the SAPC solution and then stirred for 15 h at room temperature. The concentration of the SAPC liposome was measured with a commercial kit. The sample was mixed with DMPC, DMPA, or DMPG in varying proportions, and thin films of the mixed lipids were prepared by removing the solvent. DMPC/SAPCox, DMPA/SAPCox, and DMPG/SAPCox liposomes were finally prepared.

Preparation of Aβ solution

Aβ (1-40) peptide solution was prepared from powder by dissolving in 0.2% NH_3 solution to make 200 μM of stock solution at 4°C.

Direct Observation of Growth of Aβ Fibrils with Total Internal Reflection Fluorescence Microscopy (TIRFM)

TIRFM observations were performed by a previously reported procedure.[9] Briefly, the TIRFM system used to observe the aggregation of amyloid fibril formation was developed based on an inverted microscope (IX70, Olympus,Tokyo,Japan). Aβ stock solution was diluted with Tris Buffer (pH 7.5), NaCl solution,ThT, and each liposome solution. The final solutions contained Aβ (1-40) (50 μM), Tris (50 mM), NaCl (100 mM), ThT (10 μM), and each liposome (250 or 0 μM). These samples were incubated at 37°C for more than 48 h. The ThT molecule was excited at 442 nm by a helium-cadmium laser (IK5552R-F, Kimmon,Tokyo,Japan). The laser power was 4-80 mw, and the observation period was 3–5 s. The fluorescence image was filtered with a bandpass filter (D490/30, Omega Optical, Bratteboro,VT), and visualized using a digital steel camera (DP70,Olympus).

For the estimate of number density of fibrils observed, The total internal reflection of helium-cadmium laser generated the evanescent field with about 100 nm thickness.[9] Fibrils counted up are considered to be in the evanescent field. To simply estimate the number density of nuclei and fibrils on the TIRFM system, 100 nm in thickness of evanescent layer was adopted.

Kinetic of amyloid fibril formation

The degree of aggregation of amyloid fibril formation was determined using a fluorescent dye, ThT, that specifically binds to fibrilous structures.[9,14,15] Samples contained Aβ (1-40) (5 μM), Tris (50 mM), NaCl (100 mM), and each liposome 250 or 0 μM). These samples were incubated at 37°C for more than 48 h, and the fluorescence intensity was measured at arbitrary times to investigate kinetic change. Measurements were made used Jasco FP-6500 fluorescence spectroscopy and were performed at an excitation wavelength of 444 nm and an emission wavelength of 485 nm.

Statistical analysis

All the experiment was performed by at least three times. In order to show the significant difference between data, a student *t*-test was performed.

Results and Discussion

Morphology of Aβ fibrils prepared with and without various liposomes

It is well-known that the liposome membrane can affect the fibrillogenesis of the amyloidgenic proteins.[5] Based on observations when using modified solid substrates, it has been reported that the surface state factors affecting fibrillogenesis are the hydrophobicity,[23] roughness,[23] and charge density[7] of the solid substrate. Various liposomes with different physicochemical properties were, therefore, prepared using zwitterionic/negatively-charged and the oxidized phospholipids. After the liposome (250 μM in lipid) suspension was mixed with Aβ (5 μM), the mixture was incubated at 37°C for 48 h.

The total internal reflection fluorescence microscopy (TIRFM) method combined with Thioflavin-T (ThT)[9,14–16] is a powerful tool for directly observing the morphology of Aβ fibrils, as it has been reported that the fibrils could be stained by a fluorescence probe, ThT.[24] The various morphologies of the Aβ fibrils were observed in the absence and presence of the various liposomes, as shown in Figure 1A–C. Yagi

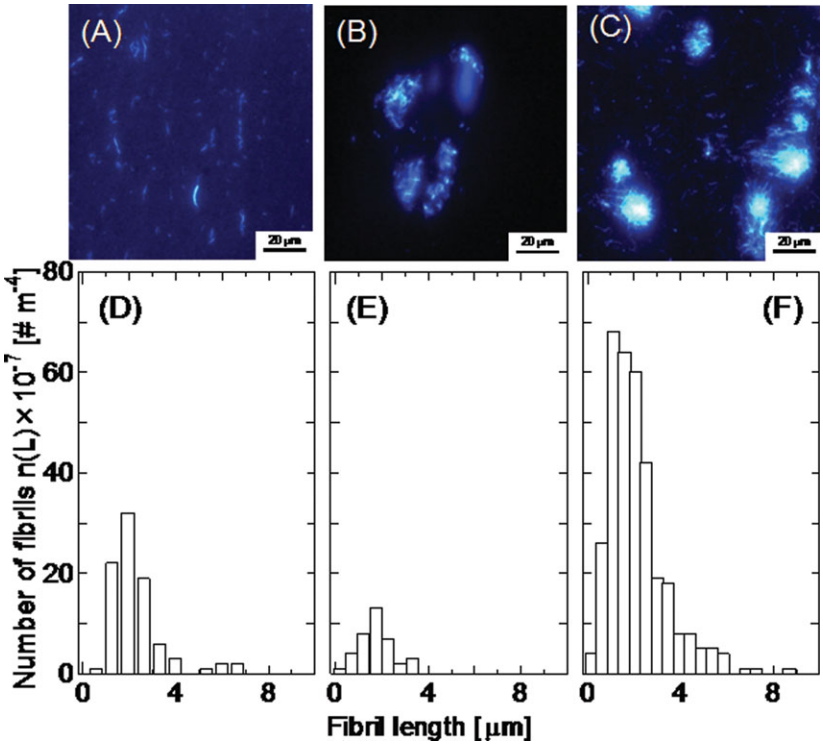

Figure 1. TIRFM image and the population density of Aβ fibrils with length L (A,D) without control, (B,E) with DMPA liposome, and (C,F) with DMPA/SAPCox (60/40 mol %) liposome.

The concentrations of Aβ(1-40) monomer and liposome were 50 μM and 250 μM, respectively. The fibril formation of Aβ(1-40) (5 μM) was performed at 37°C, pH 7.4. Evanescent layer was assumed to be 100 nm. [Color figure can be viewed in the online issue, which is available at wileyonlinelibrary.com.]

et al.[9] have reported that the morphology of the fibrils can mainly be categorized into three groups: Type I fibrils are basic straight and rigid fibrils with a diameter of ~ 10–15 nm; Type II fibrils are spherulitic amyloid assemblies of type I basic fibrils; and Type III fibrils are wormlike fibrils made of the short and rigid fibrils associated laterally.[9] The morphology formed in the presence and absence of liposomes was investigated in terms of the aforementioned criteria.

In the absence of liposome, fibrils with various morphologies such as the type I straight and rigid fibrils were observed (Figure 1A), as described previously.[19] The determined length distribution of the formed fibrils indicated that relatively long fibrils (a median length 3.1 μm) were formed, but that the number of fibrils was relatively small ($n(L)$) (Figure 1D). Some of the types of liposomes summarized in Table 1 were used to examine the effects of the addition of liposomes on the growth of fibrils and their morphology. In the presence of the zwitterionic DMPC, negatively charged DMPG) and DMPA liposomes, short laterally associated fibrils were observed (Figure 1B,E). Although these fibrils did not elongate considerably to form the worm-like fibrils (Type III), these fibrils are regarded as type III. The spherulitic amyloid assemblies (Type II) were observed in the presence of the oxidized and negatively charged DMPG/SAPCox (60/40 mol %), and DMPA/SAPCox (60/40 mol %) liposomes (Figure 1C). Based on the TEM observation, the Type II fibrils were made of the fibrils elongated from the core (data not shown). It is, therefore, difficult to evaluate the distribution of fibril length existing within spherulitic amyloid assemblies. Meanwhile, the elongation propensity of fibrils not incorporated into spherulitic amyloid assemblies would be the same as that of the type II fibrils because the fibril elongation is basically dominated by the template effect.[14,16] The length distribution of fibrils, except for the fibrils of type II, was estimated to be 2–10 μm (Figure 1F).

Table 1. Comparison of Secondary Nucleation Rate and Habits

Liposome		Habits of amyloid fibrils*	Major possible mechanism of secondary nucleation[$]	Secondary nucleation rate B [# $m^{-3}s^{-1}$]
Lipid composition	Surface state			
No liposome	-	Type I	-	$(2.83\pm0.55)\times10^5$
DMPC	Zwitterionic	Type III	(v)	$(1.35\pm0.23)\times10^5$
DMPC/SAPCox (60/40 mol%)	Zwitterionic/ Oxidized	Type III	(ii),(iv),(v)	$(1.63\pm0.21)\times10^5$
DMPG	Negatively charged	Type III	(v)	$(4.03\pm0.68)\times10^4$
DMPG/SAPCox (60/40 mol%)	Negatively charged/ Oxidized	Type II	(ii)-(iv)	$(7.63\pm1.2)\times10^4$
DMPA	Anionic	Type III	(v)	$(1.58\pm0.33)\times10^5$
DMPA/SAPCox (60/40 mol%)	Anionic/ oxidized	Type II	(ii)-(iv)	$(7.65\pm0.47)\times10^5$

*Type I: straight and rigid fibrils, Type II: spherulite, Type III is likely to include a lateral association. $ Major mechanisms on secondary nucleation are: (i) breaking, (ii) forking, (iii) diffusible, (iv) branching, (v) thickening. The B value were estimated under the experimental conditions such as Aβ(1-40) monomer: 5 μM, liposome: 250 μM, 37°C, pH 7.4, ThT: 10 μM.

It was, thus, found that the morphology of the Aβ fibrils could be varied, depending on the type of liposome membrane.

Kinetic analysis of Aβ fibrils with and without various liposomes

It has been reported that ThT specifically binds to a β-sheet structure of Aβ fibrils.[24] The fibril formation of Aβ in the presence and absence of liposomes was investigated in order to determine the factor inducing an increase in $n(L)$. As shown in Figure 2A, the final value of ThT fluorescence intensity for fibrils with oxidized liposomes indicated a definite small value as compared with those without and with nonoxidized liposome. In order to kinetically analyze the fibril growth behavior, the following function[25] was adopted

$$I(t) = I_i + m_i t + \frac{I_{\max} + m_f t}{1 + \exp\{-k(t - t_m)\}} \quad (1)$$

where t_{lag} was the lag time, k_{app} the apparent elongation rate constant, I_{i} and $I_{\max}$ the ThT fluorescence intensity at the initial and final stage, and m_{i} and m_{f} the correction factor at the initial and final stage. The t_{m} values is connected with the t_{lag} value by $t_{\text{lag}} = t_{\text{m}} - 2k_{\text{app}}^{-1}$.

The lag time corresponds to the time that requires the formation of small species of Aβ fibrils which are detectable with ThT binding assay. As shown in Figure 2B, in the absence of liposomes, the lag time was approximately 14 h. A similar lag time was observed in the presence of DMPC liposomes ($t_{\text{lag}} \sim$ 11–13 h). In contrast, the obviously accelerated effect of nucleation was observed in the presence of DMPC/SAPCox liposome ($t_{\text{lag}} \sim$ 4–6 h), which is in agreement with the accelerated nucleation caused by DMPC/SAPCox as reported by Axelsen et al.[27] The decrease in t_{lag} was also observed in the case of DMPG/SAPCox liposome. Among the possible reasons, the aforementioned accelerated effect could be caused by the strong interaction of Aβ molecule with the oxidized lipids of DMPC/SAPCox liposome.[22,26] It is considered that the accumulation of Aβ on the oxidized liposomes could surpass the critical concentration of fibril formation of Aβ ($C_{\text{crit}} \sim$ 17.6 μM [27]). Meanwhile, DMPA/SAPCox liposome showed the large t_{lag} value ($t_{\text{lag}} \sim$ 21 h), compared with DMPC/SAPCox and DMPG/SAPCox. This might result from the contribution of acidic lipid PA rather than oxidized lipids. Actually, Chauhan et al. have reported that Aβ strongly interacted with anionic phosphatidic acid (PA) liposome, in contrast to PC and PG, via the binding of Lys[28] (28th amino acid residue in Aβ molecule) with the phosphorous group of PA.[28] Meanwhile, the number of density of fibrils ($n(L)$) formed on DMPA liposomes (Figure 1E) was less than that of fibrils formed in the bulk aqueous phase (Figure 1D). It is, therefore, considered that the DMPA-Aβ interaction, which could accumulate Aβ molecules, seems to be disadvantageous for the nucleation. We considered again the possible reason on the large t_{lag} value for DMPA/SAPCox. This liposome could accumulate the large number of Aβ molecules because of the contribution of both DMPA and oxidized lipids. It is considered that the DMPA/SAPCox-Aβ interaction might require the long time to form the large number of nuclei.

On the other hand, the $I_{\max}$ value was varied, depending on the liposome type. The $I_{\max}$ value obtained in the case of oxidized liposomes was smaller value than those for the other conditions (Figure 2C). Considering the results shown in Figure 1D–F, the rapid nucleation of Aβ fibrils favored the formation of many fibrils with shorter length ($n(L)$ vs L). The addition of the oxidized liposome promoted the nucleation process prior to the fibril elongation, resulting in the production of short fibrils of Aβ. The increase in $n(L)$ between the aqueous phase and the liposome system is thought to be caused by the secondary nucleation, as described previously.[18,29] Besides, those properties might relate to the morphology of formed fibrils. Fibrils with type II favored to show the quite small $I_{\max}$ value.

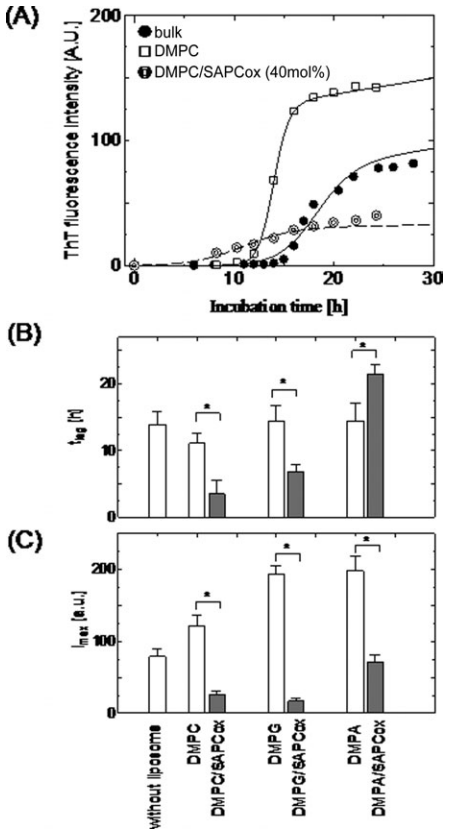

Figure 2. Kinetic analysis of amyloid fibril formation.

(A) Time-course of ThT fluorescence intensity without liposome (closed circle), with DMPC liposome (rectangle), with DMPC/SAPCox (60/40 mol %) liposome (doubled circle), (B) lag time, and (C) the maximal ThT fluorescence intensity $I_{\max}$ for various liposomes. Aβ(1-40) monomer: 5 μM, liposome: 250 μM, 37°C, pH 7.4, ThT: 10 μM. All experiments were repeated at least three times. * $p < 0.01$. All the experiments were at least triplicated.

Therefore, a mechanism of the variety of morphology of fibrils would be discussed on the kinetic parameters such as t_{lag} and $I_{\max}$. In the following, the possibility of reconsidering the function $I(t)$ by the number density of fibrils $n(L,t)$ at time t is discussed further, in order to elucidate the relationship between the fibril growth kinetics and the morphology of fibrils.

Estimate of secondary nucleation rate

In the field of crystallization, a quantification method to estimate the secondary nucleation rate, B [# m^{-3} s^{-1}], has been established. The B value is expressed by a product of the elongation rate, G [m s^{-1}] (= dL/dt), and the number density of nucleation with $L \sim 0$, n_0 [# m^{-4}][30]

$$B = G \cdot n_0 \tag{2}$$

(Note that $N(L,t) = \int_0^L n(L,t)dL$, then $n_0 = (dN/dL)_L = {}_0 = (dN/dt)_L = {}_0/(dL/dt) = B/G$). Meanwhile, there is no reasonable method to estimate the n_0 value of amyloid fibrils. In contrast, it has been reported that the estimate of the G value is subject to the surface state of the solid substrate, where the fibrils develop.[16] Another explanation for the B value is presented herein, focusing on the kinetic measurement using ThT. The fluorescence probe ThT at time t is assumed to bind to the fibrils in proportion to both the fibril length (L), and number density at time t ($n(L,t)$). Since the length and number of fibrils was increased, the observed ThT fluorescence $I(t)$ can be rewritten as a function of time t

$$I(t) = a\int_0^\infty L(t)^j n(L,t)dL \tag{3}$$

where, j is a parameter relating to the morphology of fibrils. The major objective in this study is to coarsely estimate the secondary nucleation rate B. For the simplicity, the parameter j was herein assumed to be 1. Then, the estimated $I_{\max}$ value at $t = t_f$ in Figure 2 can be described as a function of $n(L)$.

$$I_{\max} = a\int_0^\infty L(t_f)n(L,t_f)dL \tag{4}$$

The second term on the righthand side can be calculated from Figure1D–F. Thus, the proportional factor a is experimentally obtainable from Figure 1D–F and Figure 2C. The proportionality a is considered to depend on the quantum yield of ThT and its affinity to the target fibrils, although further investigations are needed. Differentiating the Eq. 3 by time t

$$\frac{dI}{dt} = a\frac{d}{dt}\int_0^\infty LndL = a\int_0^\infty \left\{Gn + L\frac{\partial n}{\partial t}\right\}dL \tag{5}$$

At the duration of $t_{\text{lag}} \sim t_{\text{lag}}+2$ (hour), the nuclei with $L\sim 0$ grows to fibrils with a length δL. The t_{lag} value is, herewith, obtainable from the Eq. 1. Therefore, the forementioned Eq. 5 can be rewritten as follows

$$\left(\frac{dI}{dt}\right)_{t=tlag\sim tlag+2} = a\int_0^{\delta L} GndL + a\int_0^{\delta L} L\frac{\partial n}{\partial t}dL$$

Note that the term on the lefthand side indicates the slope of the ThT intensity between $t_{\text{lag}} \sim t_{\text{lag}}+2$. The first term of the righthand side ($\int_0^{\delta L} GndL$) is a contribution of the elongation of each fibril to the incremental change of ThT fluorescence intensity. The second term ($\int_0^{\delta L} L\,\partial n/\partial t\,dL$) is a contribution of the increase in nuclei with a length $0\sim\delta L$ by a secondary nucleation. The integral term can be simplified if the G value is a function of L. The direct observation of a single fibril, by using the TIRFM combined with ThT, gives the time-course of fibril length (Figure 3A). The initial variation (dL/dt) corresponds to the G value (Figure 3B). The G value is found to be independent of the fibril length L (Figure 3C). Therefore, a contribution of the first term of the righthand side is considered to depend on only the number of nuclei or fibrils. We assumed, during 2 h of $t_{\text{lag}} \sim t_{\text{lag}}+2$, that a contribution of the first term can be surpassed by a contribution due to a generation of nuclei by a secondary nucleation. This is because a growth of nuclei up to δL in length being rapid (Figure 3). The aforementioned equation can, therefore, be simplified into the following equation

$$\left(\frac{dI}{dt}\right)_{t=tlag\sim tlag+2} = a\int_0^{\delta L} GndL + a\int_0^{\delta L} L\frac{\partial n}{\partial t}dL \sim a\int_0^{\delta L} L\frac{\partial n}{\partial t}dL$$

A secondary nucleation rate should be related to not only a increase in number density of nuclei but also a length L of nuclei. It should, therefore, be noted that the last integral term can be substituted by B, because the incremental change in number density of nuclei after t_{lag} is possibly due to a secondary nucleation rather than a primary nucleation. Therefore, the following equation can be obtained

$$\left(\frac{dI}{dt}\right)_{t=tlag\sim tlag+2} = a\int_0^{\delta L} L\frac{\partial n}{\partial t}dL \sim aB$$

$$\Rightarrow \quad B = \left(\frac{dI}{dt}\right)_{tlag\sim tlag+2}/a \tag{6}$$

This equation involves no influence of the surface state of the observation field and the uncertainty of the estimate of n_0 (nucleation with length $L\sim 0$). The Eq. 6 gives the coarse B value because of the following assumptions for elucidating Eq. 6: (1) the uncertainty of $n(L)$ of fibrils with submicron in length (due to the limitation of microscopic observations) was negligible; (2) a first-order dependence of L on ThT fluorescence intensity was adopted, and (3) The secondary nucleation was dominant at the time range of $t > t_{\text{lag}}$. The calculated secondary nucleation rates are summarized in Table 2, together with the secondary nucleation rate of the other materials. The order of the B value is approximately 10^4–10^5 [# m^{-3} s^{-1}], which is comparable with the previously reported results.[30,31]

Role of Oxidized Liposome on Secondary Nucleation of Aβ Fibrils

The secondary nucleation rate of Aβ fibrils in the presence of various liposomes was examined (Figure 4A). In general, the addition of DMPC, DMPG, and DMPA liposome gave a small B value. Those B values were a bit smaller than that without liposomes ($(2.83 \pm 0.55) \times 10^5$ # m^{-3} s^{-1}). This appeared to be relating to the situation, in which fibrils formed on unoxidized liposomes was likely to show the lower secondary nucleation. It was also found that the oxidized liposome favored to increase the secondary nucleation rate and the fragmentation rate constant. Especially, the DMPA/SAPCox liposome gave the largest B value ($(7.65 \pm 0.42) \times 10^5$ # m^{-3} s^{-1}). The difference in B values between the DMPA/SAPCox and the other two oxidized liposomes might have result from the Aβ-lipid interaction. As stated before, Aβ could strongly interact with PA liposome, in contrast to PC and PG liposomes.[28] According to the report by Fernandez,[32] the fibrils seems to form via the hydrogen bonding between the β-sheet of Aβs. The stability of hydrogen bonding appears to determine the stiffness of fibrils. The disruptive force would makes it possible to disrupt hydrogen bondings formed between β-sheets of Aβs in fibrils. Fibrils with a larger B value are, therefore, considered to possess a flexible structure that can be subject to mechanical stress (i.e., disruptive force).

In actual, the fragmentation rate constant of fibrils, k_f [s^{-1}], was examined by ultrasonication (Figure 4B). In any liposome

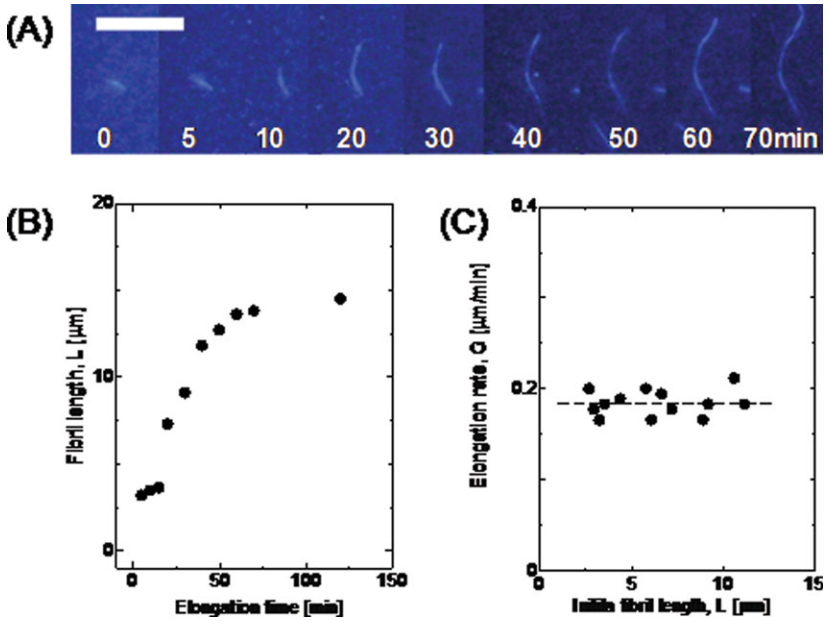

Figure 3. (A) Direct observation of growth behavior of a linear and rigid fibril, (B) time-course of changes in fibril length, and (C) relationship between the elongation rate of fibrils and their initial length Aβ(1-40) monomer: 50 μM, ThT: 10 μM. White bar represents 10 μm.

[Color figure can be viewed in the online issue, which is available at wileyonlinelibrary.com.]

with different lipids, the addition of the oxidized lipid increased the k_f value, indicating that the oxidized lipid induced the formation of fibrils with a structural advantageous for disruption. DMPC, DMPG, and their oxidized liposome system indicated a larger k_f value than that for the fibrils without liposomes. In contrast, DMPA and its oxidized liposome indicated smaller k_f values. This difference may have depended on the bulkiness of the assemblies of amyloids. In conclusion, the k_f value roughly showed the similar trends to the B value. It is considered that the secondary nucleation involved the process such that the variation in $n(L)$ could be induced by the fragmentation or other factors.

Relationship between the secondary nucleation of fibrils and their morphology

In the presence of various liposomes, the secondary nucleation rate of Aβ fibrils and their morphology (habits) as crystals were compared. The secondary nucleation rate of fibrils and their habits observed in the various conditions are summarized in Table 1. In the absence of the liposome, the linear and rigid type I fibrils were likely to show medium secondary nucleation. In contrast, the oxidized liposome system favored a larger secondary nucleation rate, resulting in the formation of type II fibrils with spherulitic amyloid assemblies.

Andersen et al.[18] have reported that the secondary nucleation mechanisms involve five different processes (1) breaking, (2) forking, (3) diffusible, (4) branching, and (5) thickening, with types (2) $\sim$ (5) being based on a nonbreaking mechanism. The B value estimated by the Eq. 6 is, in principle, based on the above mechanisms. The mode of (5) thickening involves the aggregation of filaments, protofibrils and short fibrils to form the matured fibrils, which is corresponding to the secondary nucleation. The modes of 1–4 would positively contribute to the variation of $n(L)$ against the time whereas the mode of (5) negatively. Thus, the estimation of B value determines the balance of both contributions. It has also been reported that the laser-induced destruction of fibrils (breaking) could induce fibrils of type II.[9] However, such a strong laser irradiation was never used for the observation of fibrils in this study, implying that there was no distinct contribution of the breaking mechanism (1) in fibril growth.

In the case of secondary nucleation without (1) breaking, the nonbreaking mechanisms of (2) $\sim$ (5) should be discussed. Unless fibrils have a (2) forking or (4) branching structure, the fibrils formed via the secondary nucleation would be a consequence of nucleation, which occurs laterally on the fibrils and in subsequent growth without a (3) diffusible mechanism. This mechanism ((5) thickening) would be plausible in the case of nonoxidized liposome such as DMPC, DMPA, and DMPG liposome (Figure 1B). Considering this possible mechanism in the case of nonoxidized liposome, the possible reason for medium B value in the absence of liposome was that the secondary nucleation favored not to be restricted on the surface of liposome membranes.

Table 2. Comparison of Secondary Nucleation Rate by Several Methods

	Experimental condition	Secondary nucleation rate B [#m^{-3}s^{-1}]	Ref.
Aβ fibrils	50 μM of Aβ(1-40) fibrils was observed with TIRFM to obtain the G value.	$(3.16\pm0.31)\times10^5$	This study
	ThT fluorescence intensity of Aβ(1-40) fibrils (5 μM) was monitored.	$(2.83\pm0.55)\times10^5$	This study
$AlK(SO_4)_2{\cdot}12H_2O$	Mixed suspension mixed product removal (MSMPR) -typed crystallization reactor was used to obtain the crystal.	7.44×10^7	30
Lysozyme	Crystallization with a mixed vessel under supersaturation 3.1$\sim$5.0	$10^4\sim10^7$	31

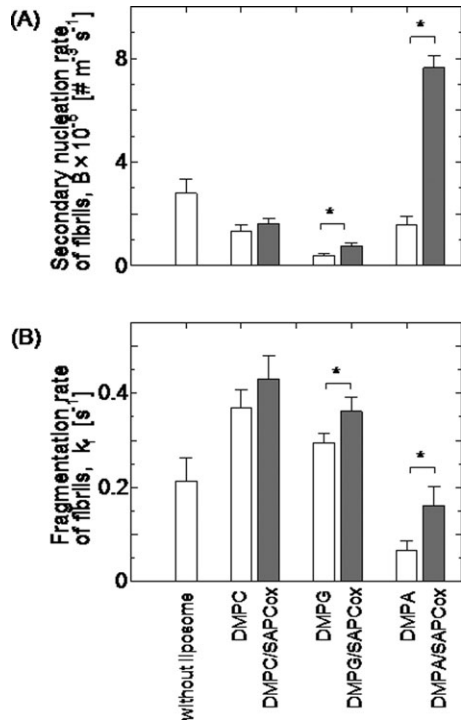

Figure 4. The effect of liposomes on (A) the secondary nucleation rate, and (B) the fragmentation rate constant.

Aβ (1-40) monomer: 5 μM, liposome: 250 μM, 37°C, pH 7.4, ThT: 10 μM. Molar ratio of lipid to oxidized lipid was 60/40 mol %. * $p < 0.01$. All the experiments were at least triplicated.

In the case of DMPC/SAPCox, diffusible, worm-like fibrils with branching were observed. Mechanisms of (2) ~ (5) might have contributed to the habits of fibrils, although the distinction of (2) forking, from (4) branching, requires a precise estimation of the line density of fibrils with a scanning TEM technique. In addition, there may have been no contribution of the mechanism (3), as no radiating growth of fibrils was observed in the presence of DMPC/SAPCox. As previously reported,[26] oxidized SAPCox lipids could promote the accelerated nucleation of Aβ molecules because of their accumulation on the membrane surface. It is, therefore, considered that such short fibrils formed on the liposomes would associate to form type III fibrils.

In addition, spherulitic amyloid assemblies were observed in the presence of DMPA/SAPCox and DMPG/SAPCox liposomes (Figure 1C). The branching/forking of fibrils and their diffusible growth was observed, although the contribution of fibril thickening was still unclear. It is, therefore, considered that the oxidized lipids might induce the branching of fibrils. PA[28] also promotes the acceleration of Aβ fibrillogenesis, similar to SAPCox.[26] Due to this effect, the number of formed nuclei would increase, consistent with the results for the $n(L)$ value for DMPA/SAPCox (Figure 1F). Negatively charged lipids such as PG suppress the elongation of fibrils on the liposome membrane,[33] implying that short fibrils or nuclei were likely to be formed. At an earlier stage, the nuclei formed on liposome would associate and aggregate to a large extent, sufficient to induce many more growth ends of assembled fibrils. This might result in the long duration of lag time for DMPG/SAPCox, and especially DMPA/SAPCox compared with DMPC/SAPCox (Figure 2B). Besides, this property might be one of factors related to the induction of the type II fibrils.

In conclusion, a coarse quantification method for the secondary nucleation rate of fibrils was developed that provided a plausible explanation of the variety of morphologies of fibrils induced in the presence of various liposomes, a process that can herewith be defined as "*Biomembrane-Mediated Crystallization*".

Acknowledgments

The author is deeply thankful to Dr. Yuji Goto and Dr. Hisashi Yagi of Osaka University for acquiring the images with a total internal reflection fluorescence microscopy and for their helpful discussion. The fundamental concept of this study was supported by the Research Group of "Membrane Stress Biotechnology" and the Sigma Multidisciplinary Research Laboratory Group (Engineering Science, Osaka University) "Membranomics". This work was partly supported by an A-STEP of Japan Science and Technology Agency (JST). Also, partly funded by the Cabinet Office, Government of Japan through its "Funding Program for Next Generation World-Leading Researchers" (No.GR066), Grants-in-Aid for Scientific Research (Nos. 21246121 and 23656525) from the Ministry of Education, Science, Sports, and Culture of Japan (MEXT), and a grant from the Global COE program "Bio-Environmental Chemistry" of the Japan Society for the Promotion of Science (JSPS).

Literature Cited

1. Hardy J, Selkoe DJ. The amyloid hypothesis of Alzheimer's disease: progress and problem on the road to therapeutics. *Science*. 2002; 297:353–356.
2. Mattson MP. Pathways towards and away from Alzheimer's disease. *Nature*. 2004;430:631–639.
3. Hall CK. Thermodynamic and kinetic origins of Alzheimer's and related diseases: a chemical engineer's perspective. *AIChE J*. 2008; 54(8):1956–1962.
4. Naiki H, Nakakuki K. First-order kinetic model of Alzheimer's β-amyloid fibril extension in vitro. *Lab Invest*. 1996;74:374–383.
5. Matsuzaki K. Physicochemical interactions of amyloid β-peptide with lipid bilayers. *Biochim Biophys Acta*. 2007;1768:1935–1942.
6. Deshpande A, Mina E, Glabe C, Busciglio J. Different conformations of amyloid induce neurotoxicity by distinct mechanisms in human cortical neurons *J Neurosci*. 2006;26:6011–6018.
7. Walsh DM, Lomakin A, Benedek GB, Condron MM, Teplow DB. Amyloid beta-protein fibrillogenesis. Structure and biological activity of protofibrillar intermediates. *J Biol Chem*. 1999;274:25945–25952.
8. Roychaudhuri R. Yang M. Hoshi MM. Teplow DB. Amyloid β-protein assembly and Alzheimer disease. *J Biol Chem*. 2009;284:4749–4753.
9. Yagi H, Ban T, Morigaki K, Naiki H, Goto Y. Visualization and classification of amyloid β supramolecular assemblies. *Biochem*. 2007;46:15009–15017.
10. Krebs MRH, MacPhee CE, Miller AF, Dunlop IE, Dobson CM, Donald AM. The formation of spherulites by amyloid fibrils of bovine insulin. *Proc Natl Acad Soc*. 2004;101:14420–14424.
11. Yagi H, Ozawa D, Sakurai K, Kawakami T, Kuyama H, Nishimura O, Shimanouchi T, Kuboi R, Naiki H, Goto Y. Laser-induced propagation and destruction of amyloid β fibril. *J Biol Chem*. 2010;285: 19660–19667.
12. Jarrett JT, Lansbury PT Jr. Seeding "one-dimensional crystallization" of amyloid: a pathogenic mechanism in Alzheimer's disease and scrapie? *Cell*. 1993;73:1055–1058.
13. Murphy RM. Kinetics of amyloid formation and membrane interaction with amyloidogenic proteins. *Biochim Biophys Acta*. 2007;1768: 1923–1934.
14. Shimanouchi T, Shimauchi N, Nishiyama K, Vu HT, Yagi H, Goto Y, Umakoshi H, Kuboi R. Characterization of amyloid-β fibrils with aqueous two-phase system: implications of fibrils formation. *Solv Extr Res Dev Jap*. 2010;17:122–128.
15. Vu HT, Shimanouchi T, Yagi H, Umakoshi H, Goto Y, Kuboi R. Catechol derivatives inhibit the fibril formation of amyloid-β peptides. *J Biosci Bioeng*. 2009;109:629–634.
16. Ban T, Morigaki K, Yagi H, Kawasaki T, Kobayashi A, Yuba S, Naiki H, Goto Y. Real-time and single fibril observation of the

formation of amyloid β spherulitic structures. *J Biol Chem.* 2006;281: 33677–33683.
17. Kotarek JA, Jhonson KC, Moss MA. Quartz crystal microbalance analysis of growth kinetics for aggregation intermediates of the amyloid-β protein. *Anal Biochem.* 2008;378:15–24.
18. Andersen CB, Yagi H, Manno M, Martorana V, Ban T, Christiansen G, Otzen DE, Goto Y, Rischel C. Branching in amyloid fibril growth. *Biophys J*. 2009;96:1529–1536.
19. Okada T, Ikeda K, Wakabayashi M, Ogawa M, Matsuzaki K. Formation of toxic Aβ(1–40) fibrils on GM1 ganglioside-containing membranes mimicking lipid rafts: polymorphisms in Aβ(1–40) fibrils. *J Biol Chem.* 2008;382:1066–1074.
20. Umakoshi H, Morimoto K, Yasuda N, Ohama Y, Shimanouchi T, Kuboi R. Development of liposome-based mimics of superoxide dismutase and peroxidase based on "LIPOzyme" concept. *J Biotechnol*. 2010;147:59–63.
21. Kotarek JA, Moss MA. Impact of phospholid bilayer saturation on amyloid-β proteinnaggregation intermediate growth: a quartz crystal microbalance analysis. *Anal Biochem.* 2010;399:30–38.
22. Shimanouchi T, Oyama E, Vu HT, Ishii H, Umakoshi H, Kuboi R. Monitoring of membrane damages by dialysis treatment: study with membrane chip analysis. *Desal Water Treatment*. 2010;17:45–51.
23. Nayak A, Dutta AK, Belfort G. Surface-enhanced nucleation of insulin amyloid fibrillation. *Biochem Biophys Res Commun*. 2008; 369:303–307.
24. Naiki H, Higuchi K, Hosokawa M, Takeda M. Fluorometric determination of amyloid fibrils in vitro using the fluorescent dye, thioflavine T. *Anal Biochem*. 1989;177:244–249.
25. Nielsen L, Khurana R, Coats A, Frokjaer S, Brange J, Vyas S, Uversky VN, Fink AL. Effect of environmental factors on the kinetics of insulin fibril formation: elucidation of the molecular mechanism. *Biochem*. 2001;40:6036–6046.
26. Koppaka V, Axelsen PH. Accelerated accumulation of amyloid β proteins on oxidatively damaged lipid membranes. *Biochem*. 2000; 39:10011–10016.
27. Sabaté R, Estelrich J. evidence of micelles in the fibrillogenesis of β-amyloid peptide. *J Phys Chem*. 2005;109:11027–11032.
28. Chauhan A, Ray I, Chauhan VPS. Interaction of amyloid beta-protein with anionic phospholipids: Possible involvement of Lys^{28} and C-terminus aliphatic amino acids. *Neurochem Res*. 2000;25:423–429.
29. Padrick SB, Miranker AD. Islet amyloid: Phase partitioning and secondary nucleation are central to the mechanism of fibrilligenesis. *Biochem*. 2002;41:4694–4703.
30. Mullin JW. *Crystallization*. 3rd ed. Butterworth Heinemann: Oxford; 1992.
31. Tait S, White ET, Lister JD. A study on nucleation for protein crystallization in mixed vessels. *Crys Growth Des*. 2009;9:2198–2206.
32. Fernández A. What factor drives the fibrillogenic association of β-sheet? *FEBS Lett*. 2005;579:6635–6640.
33. Bokvist M, Lindström F, Watts A, Gröbner G. Two types of Alzheimer's β-amyloid (1–40) peptide membrane interactions: aggregation preventing transmembrane anchoring versus accelerated surface fibril formation. *J Mol Biol*. 2004;335:1039–1049.

Manuscript received Aug. 5, 2011, and revision received Jan. 22, 2012.